Astron. Astrophys. 353, 1129–1133 (2000)

ASTRONOMY AND ASTROPHYSICS

A dense two-component plasma in a strong gravity field and thermal conductivity of neutron stars

F.V. De Blasio

Department of Physics, University of Oslo, P.O. Boks 1048, Blindern, 0316 Oslo, Norway (f.v.d.blasio@fys.uio.no)

Received 3 March 1999 / Accepted 28 September 1999

Abstract. Electron – impurity scattering in the crust of neutron stars may be a relevant mechanism in delaying the cooling and in enhancing the decay of the pulsar's magnetic field. Extending previous work, in the present note I investigate the physics of the interfaces between layers in the crust of an isolated neutron star. The calculations confirm the possible presence of high impurity concentrations and thus imply a decrease of the transport properties at low temperature.

Key words: dense matter – stars: neutron

1. Introduction

Theoretical calculations on the ground state of matter at high pressure and density indicate that the outer part of an isolated neutron star consists of a solid crust of closely packed nuclei. The temperature in the interior of the star is –except for very young stars– much smaller than $\sim E/k_B$ where E is the typical energy scale which includes the nuclear and Coulomb energy and k_B is Boltzmann's constant. As a consequence the equation of state and other properties of the crust can be calculated assuming the system in equilibrium at zero temperature. According to the equilibrium model the crust has a stratified structure consisting of a regular superposition of different layers composed by the nuclide which minimizes the total energy density.

In the present note I argue that the diffusion processes in the solid crust are very slow and prevent the system from reaching the minimal energy. The thermal distribution of nuclei (which will also be called ions) will thus reflect the situation as frozen at the melting temperature rather than at the present temperature of the star. In a preliminary study it was shown that the thermal fluctuations at the melting point produce a smearing at the interface between different layers. The impurity–rich interfaces might become efficient shields to the propagation of heat during the conductive stage of the cooling, when the crust is in the solid state (De Blasio 1998). The presence of impurities in the lattice of the solid crust might also contribute to the decay of the star's magnetic field and alter its thermal history increasing the thermal equilibration time. There are however some points in the previous paper (De Blasio 1998, hereafter Paper I) that require improved calculations and precisely:

1. The mixing entropy used to calculate the equilibrium distribution of ions is simplified with respect to more elaborate theories of two-component plasmas and essentially corresponds to the mixing entropy of an ideal solution. In addition, some simplifications were made in Paper I in order to find explicitly the expressions for the ionic composition.
2. A wrong calculation of the critical temperatures in Table 1 of Paper I affects the thickness of the mixing region as reported in the same table. It will be shown here that the effect of ionic mixing is actually much larger.
3. The conductivities in Paper I have been adopted from Flowers & Itoh (1976; 1981). More complete calculations of thermal conductivities have appeared in a recent study by Potekhin et al. (1999).

Purpose of the present paper is to improve and, when necessary, correct the previous points.

2. A dense two component plasma in a strong gravity field

The free energy density of a dense plasma composed of two ionic species labeled with "1" and "2" at temperature T in a gravity field of intensity g can be written as

$$F = F_C + E_g + F_{id} + E_{nucl} \tag{1}$$

where

$$F_C = k_B T \left[n_1 f^{OCP}(\Gamma_1) + n_2 f^{OCP}(\Gamma_2) + \Delta f \right] \tag{2}$$

is the Coulomb free energy of a ionic mixture of the two ionic species interacting with a uniform electron background,

$$E_g = m_u g \left[n_1 A_1 + n_2 A_2 \right] y \tag{3}$$

is the gravitational energy,

$$F_{id} = k_B T \Big[n_1 \ln n_1 + n_2 \ln n_2 + 3(n_1 \ln \lambda_1 + n_2 \ln \lambda_2) - (n_1 + n_2) \Big] \tag{4}$$

is the ideal part of the free energy (Landau & Lifshitz 1986) and

$$E_{nucl} = n_1 E_n(A_1, Z_1) + n_2 E_n(A_2, Z_2) \tag{5}$$

is the total nuclear energy. In Eqs. (1-5), $f^{OCP}(\Gamma)$ is the one-component plasma free energy, n_j, A_j, Z_j are the number density, mass number and charge of the ion $j = 1, 2$, $\Gamma_j = Z_j^2 e^2/r_j k_B T$ is the Coulomb parameter, r_j is the Wigner-Seitz radius of the ion j, T is the temperature, $E_n(A_j, Z_j)$ is the nuclear energy of the nuclear species j and finally m_u is the atomic mass unit. The quantity y is the height above a reference point, chosen as the one where the concentration of the two ionic species is the same, $n_1 = n_2$. The ionic thermal wavelength is

$$\lambda_j = \left(\frac{2\pi\hbar^2}{m_u A_j k_B T}\right)^{1/2}. \quad (6)$$

A useful expression for $f^{OCP}(\Gamma)$ in Eq. (2) has been published by Ichimaru (1994). More recently DeWitt & Slattery (1999) have provided the formula

$$f^{OCP}(\Gamma_j) = -0.899172\,\Gamma_j + 1.864178\,\Gamma_j^{0.323064} - 0.274823\,\ln\Gamma_j - 1.4018. \quad (7)$$

In Eq. (7) the first term is by far the dominant one. It accounts for about 96% of the total Coulomb free energy at the melting point and its derivative gives 98% of the energy. Thus, in the present paper only this term will be included in the calculations. Note that the interaction energy of a uniform spherical charge Z distributed within a sphere of radius r (which for a one-component plasma is the Wigner-Seitz radius) with a point like charge in the centre is $-(9/10)\,Z^2e^2/r = -0.90\,\Gamma\,k_BT$ which would be already quite accurate for the present calculation. The deviation Δf from the pure mixing rule in Eq. (2) is very small compared with the rest of the free energy (DeWitt et al. 1996) and will be neglected. The nuclear energy in Eq. (5) is completely negligible in the present problem as will be shown at the end of this section.

The condition of charge neutrality for the two-component plasma is

$$n_1 Z_1 + n_2 Z_2 = n_e \quad (8)$$

where n_e is the electron number density. To calculate the ionic distribution at equilibrium one can minimize the free energy, Eq. (1) using n_1, n_2 or their ratio as variable. The electron number density is assumed to depend linearly on the distance y

$$n_e(y) \approx n_e(0) + Ly \quad (9)$$

where $L = (\partial n_e/\partial y)_{y=0}$. All the functions depending on $n_e(y)$ are linearized accordingly.

Minimizing the free energy in Eq. (1) and using Eqs. (2–9) I find

$$k_B T_m \Xi = \Lambda y \quad (10)$$

where following the introductory discussion the temperature is fixed at the melting point $T = T_m$, and a global additive constant has been fixed to give $n_1 = n_2$ for $y = 0$. In Eq. (10), Λ is the restoring force acting on a displaced ion

$$\Lambda = 0.482\left|n_e(0)^{-2/3}L\right|e^2 Z_1 Z_2 (Z_1^{2/3} - Z_2^{2/3}) + m_u g(A_1 Z_2 - A_2 Z_1) + \frac{(Z_2 - Z_1)k_B T_m L}{n_e(0)} \quad (11)$$

Table 1. Properties of the interfaces from Haensel & Pichon (1994). Each entry denotes the density (g cm^{-3}), the pressure (erg cm^{-3}), the charge and the mass number of the lower and of the upper nucleus, the melting temperature of the lower and upper layer (in 10^9 K) and the total thickness W (in cm). All the data presented in the paper have been obtained for a gravity field of intensity 2×10^{14} cm s^{-2}.

Log(ρ)	Log P	Z_1	A_1	Z_2	A_2	T_1	T_2	W
9.36	27.05	36	86	28	66	0.51	0.34	671
9.85	27.68	34	84	36	86	0.67	0.74	452
10.99	29.16	28	78	30	80	1.11	1.24	630
11.05	29.49	44	126	28	78	2.46	1.17	1211
11.20	29.90	42	144	44	146	2.40	2.62	958

and Ξ is given by

$$\Xi = -Z_2 \ln\eta + (Z_2 - Z_1)\ln\left(\frac{Z_1 + Z_2}{\eta Z_1 + Z_2}\right) = \ln\left[\left(\frac{1+R}{1+\eta R}\right)^{Z_1}\left(\frac{1+\eta^{-1}R^{-1}}{1+R^{-1}}\right)^{Z_2}\right] \quad (12)$$

with $\eta = n_1/n_2$ and $R = Z_1/Z_2$. For $\eta << 1$ the solution behaves like

$$\eta \approx (1 + R^{-1})\exp(1-R)\exp\left(\frac{-\Lambda y}{Z_2 k_B T}\right). \quad (13)$$

The derivative of the electron number density at the second member of Eq. (11) can be written as

$$n_e(0)^{-2/3}|L| = \left[\frac{\langle Z\rangle\,\rho}{\langle A\rangle\,m_u}\right]^{1/3}\frac{\rho g}{\gamma P} \quad (14)$$

where P is the pressure, $\langle A\rangle$ and $\langle Z\rangle$ are the average nuclear mass and charge and $\gamma = (\rho/P)\partial P/\partial\rho$ is the adiabatic index.

Studies of the equilibrium phase diagram of binary dense plasmas (Ichimaru 1994, Chabrier & Potekhin 1998) show that if the charges of the two ionic species are not very different, the melting temperature changes linearly as a function of the composition $x = n_1/(n_1 + n_2)$. The local melting temperature is thus calculated with the expression

$$T_m(x) \approx T_m(0)[1 + x(R^{5/3} - 1)]. \quad (15)$$

For the calculations I use the equation of state and composition proposed by Haensel & Pichon (1994) based on nuclear experimental energies.

The relevant data for the calculations are collected in Table 1 where the index "1" denotes the ions that occupy the region at higher density. Fig. 1 shows the behavior of the ratio $x = n_1/(n_1 + n_2)$ as a function of the distance y. The convention adopted here is that $y > 0$ for the small density region. The five densities considered are $\rho = 2.3 \times 10^9$ g cm^{-3}, $\rho = 7.0 \times 10^9$ g cm^{-3}, $\rho = 9.6 \times 10^{10}$ g cm^{-3} $\rho = 1.1 \times 10^{11}$ g cm^{-3} and $\rho = 1.6 \times 10^{11}$ g cm^{-3}. It is evident that the composition varies smoothly between two zones in the crust. From Eq. (13) the thickness of the mixed region scales like $W \approx k_B\,\langle Z\,T_m\rangle\,/\Lambda$. The values of W for the five density regions have been extracted

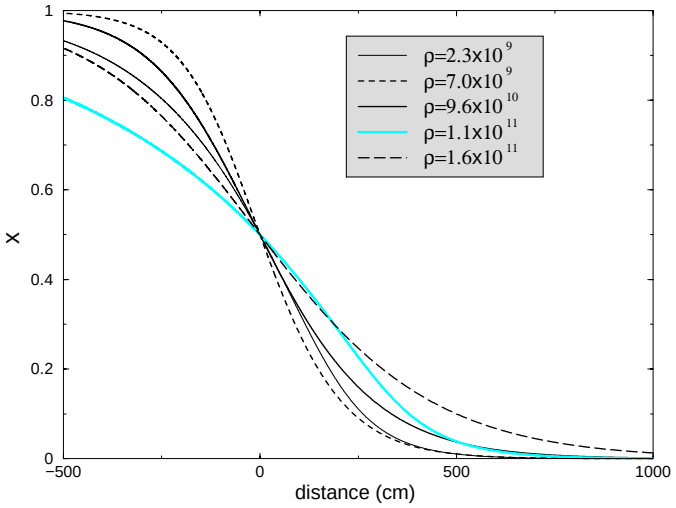

Fig. 1. The fraction of one ionic species, $x = n_1/(n_1 + n_2)$ is shown as a function of the distance from the middle of the interface for five different density regions.

from the numerical solution, Eq. (12) and reported in Table 1. They result to be of the order 400–1200 cm.

Note from Table 1 that in the second, third and the last of the densities considered, both the mass and proton numbers are larger for the nucleus at the top. Since nuclei with larger masses and charges tend to settle to the bottom there might appear to be a problem of mechanical instability in the sequence of nuclei as calculated not only by Haensel & Pichon (1994) but also in previous work (Baym et al. 1971). Obviously this is not so. In the gravitative term, which is the largest contribution to the force acting on an ion (see Eq. (11)), the nuclear parameters appear in the combination $A_1Z_2 - A_2Z_1$, where the label 1 denotes the lower ion. This quantity is always positive ensuring the stability of the system. For jumps of two protons and constant neutron number as in the examples considered the above combination simply gives twice the neutron number.

Fig. 1 shows that the distribution of impurities extends far beyond $\sim W/2$. The total effective thickness of mixed lattice where a modification of the thermal conductivity can be expected, reaches in some cases values as large as ~ 20 m. Even if this value is still much smaller than the thickness of a whole layer in the crust ($\sim 30 - 100$ m) the transport properties can be modified markedly, as shown in Sect. 3. Note that the values of the thickness of the mixed phase reported in Table 1 of Paper I are smaller compared to what found here. This is partly due to the different charges and of the equation of state adopted in Paper I and in part to the fact that the displacements ξ in Paper I have been calculated from erroneous values of the melting temperatures. The correct values for the temperatures are reported in Table 1 of the present paper. As a general conclusion the effect is actually larger than what indicated in Table 1 of Paper I.

I now discuss the contribution from the nuclear energy in Eq. (1). In principle the nuclear energy is very important in the energy balance of the crust. Differences in the models describing the physics of neutron-rich nuclei can have large effects in modelling the composition of the crust. It will be shown in the remainder of this section that the nuclear part of the free energy does not play an important role in the present calculations. Accounting for the nuclear energy would require to add a term of the form $[\partial(E_1Z_2 - E_2Z_1)/\partial y_{y=0}]$ at the second member of Eq. (11). The essential point is that one has to consider the change in the nuclear energy when a nucleus moves vertically through the ambient electron gas and not the nuclear energy itself. Let us consider a nucleus drifting downwards into the star. The increase of the electron density in the nuclear region causes the effective charge of the nucleus to decrease. The nuclear Coulomb energy becomes smaller while the proton kinetic energy increases due the compression of the proton distribution. All the relevant forms of nuclear energy change because of the strong neutron-proton interaction. The overall effect can be treated approximately allowing for a total change of the nuclear charge in the following fashion

$$Z^2e^2 \to (Z^2e^2)_{eff} = Z^2e^2\left[1 - \frac{V_N n_e}{Z}\right]^2 \tag{16}$$

where V_N is the volume of the nucleus. Using a Hartree-Fock numerical code with Skyrme III force parameters I calculate the change in the total nuclear energy ΔE when n_e is increased of a fixed quantity $\Delta n_e = L\Delta y$ corresponding to a vertical displacement Δy. Considering the physical quantities at a density $\rho = 9.64 \times 10^{10}$ g cm^{-3} I find a force of the order $\approx 10^{-4}$MeV cm^{-1}, between two to three orders of magnitude smaller than the electromagnetic plus gravitational force. Finally in Eq. (1) a term in the free energy due to electron screening has also been neglected. This term is in fact important only at the lowest densities not considered in the present paper (Chabrier & Potekhin 1998).

3. Thermal conductivity of neutron stars

The total conductivity k in the crust is given by

$$1/k = 1/k_i + 1/k_{imp} + 1/k_{ee} \tag{17}$$

where k_i, k_{imp} and k_{ee} are the conductivities resulting only from electron–ion, electron–impurity and electron–electron scattering. The electron-electron conductivity is much larger than the ionic conductivity and following Potekhin et al. (1999) the quantity k_{ee}^{-1} will be neglected in Eq. (17).

In Paper I, I adopted the conductivities as calculated by Flowers & Itoh (1976; 1981). Important physical effects neglected in the previous works have been included in the calculations by Yakovlev & Urpin (1980), Itoh & Kohyama (1993) and more recently by Baiko et al. (1998) and Potekhin et al. (1999). The most recent very accurate calculations which are adopted here take into account the nuclear form factor due to the finite size of the nuclei and the phonon reduction of electron-ion scattering through the Debye-Waller factor.

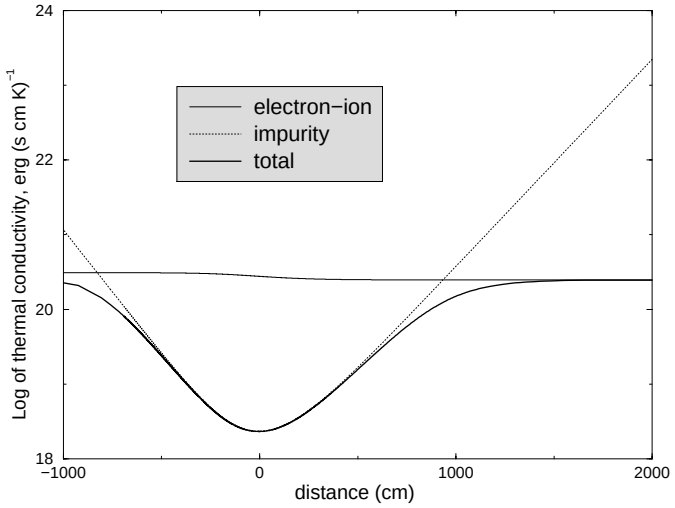

Fig. 2. The electron-ion, impurity and total thermal conductivity as a function of the distance from the middle of the interface for the density zone $\rho = 9.6 \times 10^{10}$ g cm^3. The temperature is $T = 10^6$ K.

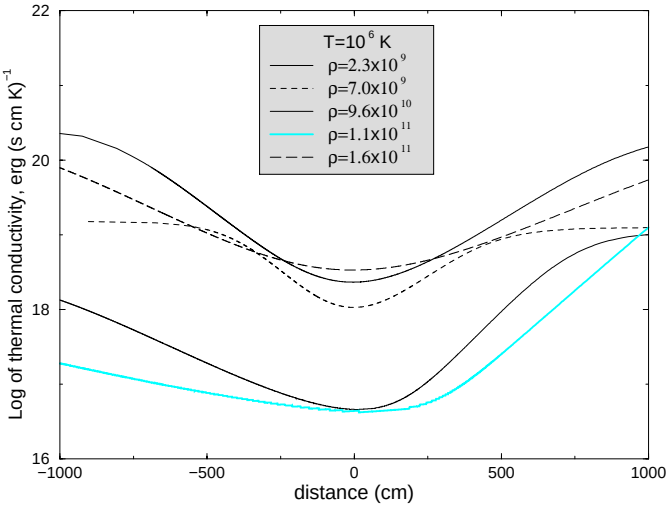

Fig. 3. The total thermal conductivity at temperature $T = 10^6$ K for the density zones indicated.

The electron-ion thermal conductivity can be written in terms of the effective collision frequency for the electron-ion scattering ν_i as (Potekhin et al. 1999)

$$k_i = \frac{\pi^2 k_B T n_e}{3 m^* \nu_i} \tag{18}$$

where the frequency is given as

$$\nu_i = \frac{4\alpha^2 Z \epsilon_F \Lambda_c}{3\pi\hbar}. \tag{19}$$

In Eqs. (18–19) α is the fine structure constant, ϵ_F is the electron Fermi energy and Λ_c is the Coulomb logarithm for the thermal conductivity (Yakovlev & Urpin 1980). The variable $m^* = m_e(1+(\hbar k_F/m_e c)^2)^{1/2}$ is the relativistic electron mass, where m_e is the bare mass and k_F the electron Fermi wave number. The Coulomb logarithm is calculated after Potekhin et al. (1999). The expression for impurity conductivity which is taken from Itoh & Kohyama (1993) can be written in the form

$$k_{imp} = G(x)\left(\frac{\langle Z\rangle}{\Delta Z}\right)^2 \frac{1}{x(1-x)} \tag{20}$$

where $G(x)$ is a function of the density, ionic masses and charges and which depends weakly on the impurity fraction $x = n_1/(n_1+n_2)$. The relevant factors displayed in Eq. (20) show explicitly that the resistivity is proportional to the square of charge fluctuation ΔZ and to the factor $x(1-x)$. A reduction of the conductivity can be expected for strong charge fluctuations and when the two ionic species have comparable concentrations.

Fig. 2 displays the total thermal conductivity k, the electron-ion conductivity k_{ie} (which would represent the total conductivity in the absence of the effect proposed in the paper) and the impurity conductivity k_{imp} as a function of y. The density is fixed at $\rho = 1.3 \times 10^9$ g cm^{-3} and the temperature is 10^6 K. The net effect is a decrease of the thermal conductivity of about two orders of magnitude.

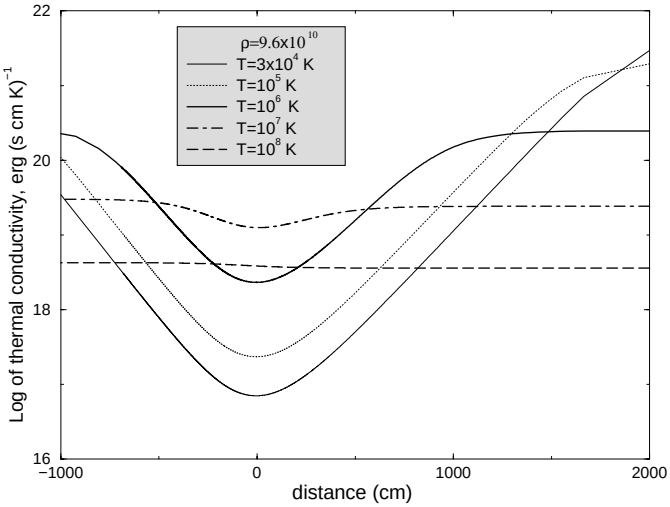

Fig. 4. The total thermal conductivity at the density region $\rho = 9.6 \times 10^{10}$ g cm^{-3} for different temperatures.

The total conductivity for the other density zones is shown in Fig. 3 for a temperature of 10^6 K. Note how the different interfaces produce quite diverse effects. For example, the effect at a density $\rho = 1.6 \times 10^{11}$ g cm^{-3} is almost negligible at this temperature, while at the interface $\rho = 1.1 \times 10^{11}$ g cm^{-3} the conductivity drops of more than two orders of magnitudes for a total length of more than twenty meters. Main responsible for this huge effect is the large charge difference between the two neighboring nuclei. According to the calculations by Haensel & Pichon (1994) this is the largest charge jump in the whole outer crust.

In Fig. 4 different temperatures are presented for the density region $\rho = 9.6 \times 10^{10}$ g cm^{-3}. At a temperature below 10^6–10^5 K the effect becomes of great importance while it is essentially negligible for temperatures larger than 10^7 K.

Protoneutron stars and young neutron stars emit energy mainly via modified URCA processes in the interior. At a later

stage, the main cooling mechanism is photon emission from the star's surface. At the beginning the temperature profile depends on the local emissivities, until after $\sim 10\,yr$ from the birth of the star the thermal conduction becomes efficient to make the temperature more uniform. After $\sim 10^4$–10^5 yr the internal temperature is about 10^7 K. It is at this stage that the mechanism proposed in the paper might become effective. Recent observations from ROSAT seem to favor standard cooling with respect to the various fast cooling scenarios. It is expected that the presence of impurities, enhancing the thermal equilibration time, may delay even further the cooling of the star. This might open more room for fast cooling scenarios (Page 1998). Due to the variability of the physical properties between the surface and the interior, the process of thermalization involves the whole crust and should be calculated making proper use of a complete cooling code. Estimates performed in Paper I where the single interfaces are considered separately are purely indicative. Finally, the presence of large concentrations of impurities will also change the relation between the internal and the surface temperature of a cooling neutron star and to some extent alter the evolution of the pulsar magnetic field.

Acknowledgements. The subroutine for the calculation of the Coulomb logarithms was provided by A. Potekhin, whom I also thank for useful comments on Paper I. Thanks to V. Urpin for useful suggestions during the completion of Paper I are extended to the present work. An anonymous reviewer improved considerably the quality of the article. The work was sponsored by the Marie Curie Research Training Grant under contract ERB4001GT96383G.

References

Baiko D.A., Kaminker A.D., Potekhin A.Y., Yakovlev D.G., 1998, Phys. Rev. Lett. 81, 5556
Baym G., Pethick C.J., Sutherland P., 1971, ApJ 170, 299
Chabrier G., Potekhin A.Y., 1998, Phys. Rev. E 58, 4941
De Blasio F.V., 1998, MNRAS 299, 118 (Paper I)
DeWitt H., Slattery W., Chabrier G., 1996, Physica B 228, 21
DeWitt H., Slattery W., 1999, Contrib. Plasma Phys. 39, 97
Flowers E., Itoh N., 1976, ApJ 206, 218
Flowers E., Itoh N., 1981, ApJ 250, 750
Haensel P., Pichon B., 1994, A&A 283, 313
Itoh N., Kohyama Y., 1993, ApJ 404, 268
Ichimaru S., 1994, Statistical Plasma Physics Vol. 2: Condensed Plasmas. Addison Wesley, Reading
Landau L.D., Lifshitz E.M., 1986, Statistical Physics. Part I, Pergamon, Oxford
Page D., 1998, Thermal Evolution of Isolated Neutron Stars. In: Shibakazi N., Kawai N., Shibata S., Kifune T. (eds.) Neutron Stars and Pulsars. Universal Academy Press, Tokyo, p. 183
Potekhin A.Y., Baiko D.A., Haensel P., Yakovlev D.G., 1999, A&A 346, 345
Yakovlev D.G., Urpin V.A., 1980, SvA 24, 303